Remote Sensing of Environment 205 (2018) 32–45

Contents lists available at ScienceDirect

Remote Sensing of Environment

journal homepage: www.elsevier.com/locate/rse

Analyzing spatial and temporal variability in short-term rates of post-fire vegetation return from Landsat time series

Ryan J. Frazier[a,*], Nicholas C. Coops[a], Michael A. Wulder[b], Txomin Hermosilla[a], Joanne C. White[b]

[a] Integrated Remote Sensing Studio, Department of Forest Resources Management, University of British Columbia, 2424 Main Mall, Vancouver, British Columbia V6T 1Z4, Canada

[b] Canadian Forest Service (Pacific Forestry Centre), Natural Resources Canada, 506 West Burnside Road, Victoria, British Columbia V8Z 1M5, Canada

ARTICLE INFO

Keywords:
Boreal
Forest
Recovery
Regeneration
Disturbance
Landsat: Time series
Ecozone
Taiga
Shield

ABSTRACT

The disturbance and recovery cycles of Canadian boreal forests result in highly dynamic landscapes, requiring continued monitoring to observe and characterize environmental change over time. Well-established remote sensing methods capture change over forested ecosystems, however the return of forest vegetation in disturbed locations is infrequently documented and not well understood. Landsat time-series data allows for both the capture of the initial disturbance and the ability to monitor the subsequent vegetation regeneration with spectral vegetation indices. In this research, we used three spectral recovery metrics derived from an annual Landsat-based per-pixel Normalized Burn Ratio time series to determine trends in the short-term rates of spectral recovery for areas disturbed by wildfire (1986–2006), as assessed using a series of 5-year post-disturbance windows to observe forest recovery trends. Our results indicated that rates of spectral forest recovery vary over time and space in the Taiga and Boreal Shield ecozones. We found evidence that post-fire spectral forest recovery rates have accelerated over time in both the East and West Taiga Shield ecozones, with a consistent, positive, and significant trend measured using a Mann-Kendall test for monotonicity and Theil-Sen slope estimation. Over the analysis period (1986–2011), relative rates of spectral forest recovery increased by 18% in the Taiga Shield East and 9% in the Taiga Shield West. In contrast, spectral forest recovery rates in the Boreal Shield varied temporally, and were not consistently positive or negative. These results demonstrate that post-fire spectral recovery rates are not fixed over time and that spectral trends are dependent upon spatial location in the Canadian boreal. This retrospective baseline information on trends in spectral recovery rates highlights the value of, and continued need for detailed monitoring of vegetation regeneration in boreal forest ecosystems, particularly in the context of a changing climate.

1. Introduction

Climate and disturbance are the two most important factors that shape the Canadian boreal landscape (Brandt et al., 2013). First, climate primarily controls where and which tree species grow and adapt in forested areas, with annual tree growth limited by short growing seasons and severe winters (Gauthier et al., 2015). Second, disturbances drive change in the boreal, particularly fires, which occur frequently over large areas, and are critical for many ecosystem functions (Stocks et al., 2002). As a result of the interplay between climate and disturbance, Canadian boreal forest ecosystems are a mosaic of patches with varying age, structure, biodiversity, productivity, and species composition (Weber and Flannigan, 1997). Thus, boreal tree species have adapted to frequent disturbance by utilizing multiple post-disturbance recovery methods, which occur over relatively long periods of time. This post-disturbance recovery period is 1) a critical time to monitor the reestablishment and health of boreal forests (Gauthier et al., 2015), and 2) highly susceptible to changes in climate. Any disruption of the recovery process can in turn impact the essential ecosystem goods and services provided by boreal forests (Brandt et al., 2013; Gauthier et al., 2014; Gauthier et al., 2015).

Boreal forests are expected to be altered extensively by a changing climate (Brandt et al., 2013; Price et al., 2013; Gauthier et al., 2014; Gamache and Payette, 2004). Currently, boreal ecosystems are undergoing alterations in phenology (Lemprière et al., 2008; Colombo, 1998), productivity (Nemani et al., 2003; Jarvis and Linder, 2000), and disturbance (Stocks et al., 1998; Flannigan et al., 2000; Flannigan et al., 2005; Johnstone et al., 2010), all attributed to changes in climate. With

* Corresponding author.
E-mail address: rfrazier@alumni.ubc.ca (R.J. Frazier).

https://doi.org/10.1016/j.rse.2017.11.007
Received 7 June 2016; Received in revised form 3 November 2017; Accepted 10 November 2017

respect to altered disturbance characteristics, a changing climate has had mixed effects on forest recovery as well. For example, three key tree species within the Canadian boreal forest have shown divergent responses to a changing climate. Black spruce (*Picea mariana*) dominated systems showed an increase in growth under cooler and wetter conditions (Girardin et al., 2016; Brooks et al., 1998), while jack pine (*Pinus banksiana*) ecosystems displayed increased growth with warmer temperatures and increased spring precipitation (Brooks et al., 1998). Additionally, white spruce (*Picea glauca*) trees have reacted positively to warmer spring temperatures with increased annual growth, but also negatively to much warmer summers with decreased annual growth (Wilmking et al., 2004) that is likely caused by a lack of available moisture (Barber et al., 2000; D'Orangeville et al., 2016).

Spatially extensive temporal trends describing increasing or conversely decreasing vegetation quantity and vigor have been found occurring across the Canadian boreal using coarse (100–1000 m) grained remotely sensed data. Both increasing and decreasing spectral trends have been detected occurring over Canadian boreal forests over time (Pouliot et al., 2009) dependent on location, and those trends are well correlated with trends found at coincident smaller spatial resolution (30 m) data (Olthof et al., 2008). However, some of the spectral trends found at coarse scales have also been shown to be influenced by the inter-instrument calibration, sensor drift, and preprocessing steps (Alcaraz-Segura et al., 2010). Moreover, coarse spatial resolution studies can fail to capture the fine scale mosaicked nature of the boreal forest landscape and are often in disagreement with research done at finer spatial scales (Alcaraz-Segura et al., 2010; Fraser et al., 2011; Wulder et al., 2010). In contrast to known issues with inter-instrument calibration of broad-scale sensors (Alcaraz-Segura et al., 2010), finer spatial resolution Landsat data (30 m) has fewer inter-sensor calibration issues (Markham and Helder, 2012; Vogelmann et al., 2016), although issues regarding inter-sensor calibration of certain spectral wavelengths are noted to exist (Sulla-Menashe et al., 2016; Ju and Masek, 2016).

Finer grained medium spatial resolution (30–100 m) remotely sensed data have also shown some broad spectral trends derived from time series of spectral indices, and importantly have been previously tied to physical properties of forests (Pouliot et al., 2009, McManus et al., 2012, Chu and Guo, 2013, Fraser et al., 2014a, 2014b). For example, the Normalized Difference Vegetation Index (NDVI) is a spectral index that has often been used to examine active photosynthetic vegetation quantity and is linked to forest condition changes over time at broad spatial scales (Cuevas-González et al., 2009; McManus et al., 2012; Turubanova et al., 2015). While some have found a widespread NDVI derived trend of increasing vegetation over time that is associated with a thickening canopy (Myneni et al., 1997, Slayback et al., 2003, Olthof and Latifovic, 2007), Goetz et al. (2005) found that Canadian boreal forests experienced a negative trend between 1981 and 2003 related to reductions in vegetation abundance (Beck and Goetz, 2011; Bi et al., 2013). Often applied more commonly in fire severity studies, the Normalized Burn Ratio (NBR) spectral index and its change over time have been linked to forest structural properties (Wulder, 1998, Epting et al., 2005, Schroeder et al., 2011), and may be more suitable than NDVI for forest recovery tracking (Pickell et al., 2016; Buma, 2012).

Detailed and annual forest recovery information over large areas can be derived from fine spatial resolution wall-to-wall remotely sensed datasets, principally due to free and open data access, data storage, and processing capacity (Kennedy et al., 2014). The United States Geological Survey maintains the Landsat data archive and provides an ideal data set for boreal-wide research that offers a well-calibrated data record initiated in 1972 with complete spatial coverage in fine detail (Wulder et al., 2012; White and Wulder, 2014). Larger areas and longer time periods of spectral data can now be used to inform on the finely detailed process of forest recovery, especially after the wildfire-caused stand replacing disturbances that are typical of the Canadian boreal. For example, Pickell et al. (2016) used Landsat time series analysis across a range of forested boreal bioclimatic zones and observed differing spectral forest recovery rates for each zone. Likewise, Frazier et al. (2015) examined spectral forest recovery using Landsat time series data and found a relationship between spectral recovery differences related to distinct forest recovery processes across two ecozones.

In summary, while research has indicated that boreal forest recovery rates vary spatially (Schroeder et al., 2007; Frazier et al., 2015) and temporally (Chu and Guo, 2013), changes in the post-disturbance forest recovery rates over time has been less well examined (Ju and Masek, 2016; Goetz et al., 2006). In this study, we examine boreal forest recovery rates following wildfire during a period of changing climate to determine how recovery rates have changed over a 26-year long period, both temporally and spatially. We focus on the Boreal and Taiga Shield ecozones as representing nearly half of the Canadian boreal zone, ensuring a wide array of boreal forest conditions and fire severities are considered. The 3,013,995 km^2 study area and wall-to-wall mapping offer the ability to compare all observed forest fire disturbances and their subsequent recovery. To do so we: 1) use multiple spectral forest recovery metrics derived from Landsat time series data to inform on different aspects of post-fire spectral recovery; 2) detect trends in post-fire spectral forest recovery rates first at a 100 km cell spatial unit to visualize detailed trend patterns; 3) understand broad environmental change by using ecozone analysis units to detect spectral recovery rate trends; and, (4) determine if statistically significant trends in spectral recovery rates exist over time. Significant results are then discussed in relation to the disturbance and recovery regimes of Canadian boreal forests, as well as the benefits and limitations of spectral forest recovery metric approaches used in this study.

2. Materials and methods

2.1. Study area

Our study area covers the forested boreal areas with the Canadian Boreal Shield and Taiga Shield ecozones (Fig. 1; Ecological Stratification Working Group, 1996, Brandt, 2009). For scientific analyses and due to differences in climate and disturbance regimes, the Boreal Shield and Taiga Shield ecozones are often divided into eastern and western sections (Andrew et al., 2012; Bolton et al., 2015). Eastern sections generally experience a less harsh winter and more annual precipitation when compared to the western counterparts (Kurz et al., 1992; Kull et al., 2006; Frazier et al., 2015). Both western ecozone sections experience more forest fires (Stocks et al., 2002); forest harvesting occurs in all ecozones, and insect infestations play a larger role in eastern than western disturbance regimes (Brandt et al., 2013). Forest fires have affected 25,039,523 ha or 9.9% of the study area between 1985 and 2010 (White et al., 2017). When combined together, these two ecozones account for 49% of the Canadian Boreal zone (Brandt, 2009).

The West and East Boreal Shield ecozones are dominated by forests and characterized by many small lakes and streams interspersed between rocky outcrops with rolling and hilly topography. A precipitation gradient exists varying from higher (1000 mm per year) amounts in the coastal east, and lesser (400 mm per year) in the continental west. January mean temperatures are − 20 °C and − 1 °C in the west and east showing a pronounced colder west to warmer east temperature gradient (Urquizo, 2000), and the mean annual temperature is approximately 3 °C. Boreal Shield forests are dominated by black and white spruce stands, with southerly portions having a wider mix of broadleaf and coniferous species, i.e. white birch (*Betula papyrifera*), trembling aspen (*Populus tremuloides*), white (*Pinus strobus*), red (*Pinus resinosa*) and jack pine (Ecological Stratification Working Group, 1996).

Located north of the Boreal Shield Ecozones, the Taiga Shield Ecozones are physically divided by Hudson Bay. The topography is marked by rolling uplands punctuated by rocky outcrops, and glacial moraines and eskers. Differences in temperature and precipitation

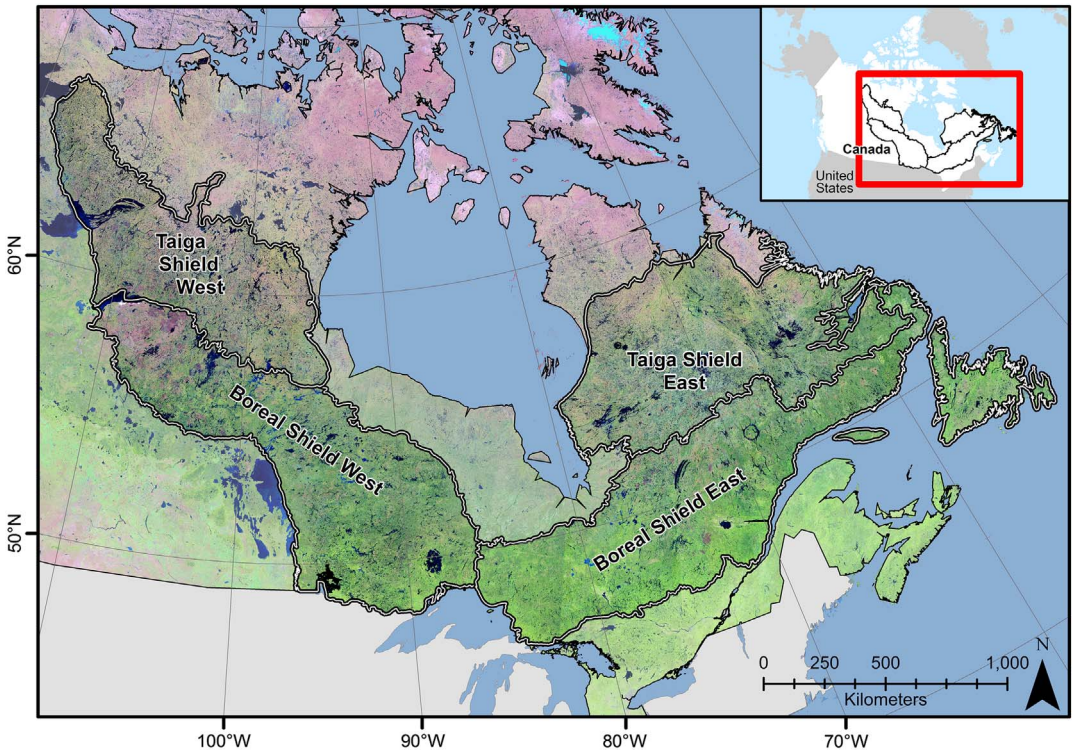

Fig. 1. The study area is displayed with a false colour Landsat composite (R; Band 5, G: Band 4, B: Band 3). The four ecozones under study are displayed: the East and West sections of the Boreal and Taiga Shield. The featured ecozone areas are also restricted to the Boreal ecosystem as defined by Brandt (2009).

reflect the coastal eastern and continental western sections; the eastern portion receives 500–800 mm per year of precipitation and experiences a milder winter with mean January temperatures near − 11 °C. Annual precipitation in the Taiga Shield West range is (300–600 mm) lower than the eastern section, and average January temperatures are − 25 °C. The northern edge of the Taiga Shield delineates the edge of where tree growth is possible; however, common throughout the ecozone are forest stands dominated by short black spruce and jack pine, with white spruce dominated mixed wood stands including balsam fir (*Abies balsamea*), trembling aspen, balsam poplar (*Populus balsamifera*), and white birch (Ecological Stratification Working Group, 1996).

2.2. Spectral data

Annual, cloud-free, and spatially seamless surface reflectance image composites and change products derived from Landsat Thematic Mapper (TM) and Enhanced Thematic Mapper Plus (ETM +) data were utilized for this analysis, representing the period 1984–2012 (Hermosilla et al., 2016; Hermosilla et al., 2015a; Hermosilla et al., 2015b). The Composites-to-Change (C2C) algorithm was applied to produce these data and is briefly described here. First, annual best-available-pixel (BAP) spectral composites were produced using all peak growing season imagery (White et al., 2014) and then the NBR spectral index was calculated (Key and Benson, 1999). A temporal segmentation algorithm was then applied to the NBR time series to determine and quantify change over time and to infill data gaps with proxy spectral values (Hermosilla et al., 2015a). Importantly, the NBR spectral index ranges between 1 and − 1, with low values indicating low or no vegetation present, while high values are known to represent dense healthy vegetation. NBR has been successfully used to: 1) assess burn severity of fires (French et al., 2008); 2) detect and classify forest disturbances (Wulder et al., 2009), and; 3) inform on forest attributes (Pflugmacher et al., 2012; Frazier et al., 2014). Lastly, regions that underwent change were geometrically, temporally and spectrally characterized, and then classified by change type. Hermosilla et al. (2015b) found their C2C methods to be accurate over the forested area of Saskatchewan and reported user's and producer's accuracy for wildfire of 97.8% and 96.7%, respectively.

2.3. Methods

2.3.1. Data stratification and filtering

Analysis of spectral forest recovery rate trends was first undertaken at a 100 km grid cell scale to ascertain if there were any spatial patterns in spectral forest recovery trends within the ecozones themselves. The use of the 100 km grid cells allowed for the collection of spectral recovery rate data over a long periods and discrete areas, and allow the results to be more efficiently reported and shared. After the 100 km grid cells were analyzed, then each ecozone analysis unit was analyzed as a whole to determine if spectral forest recovery rates showed a consistent trend over time. In order to better capture the initial signs that can indicate forest recovery is possible, the Landsat time series data were filtered such that only spectral recovery trajectories from moderate and high severity fires (typically stand replacing fires) were considered (Fig. 2). Fires were selected using a threshold value of NBR change (dNBR) that represented a level of severity high enough to initiate the growth of a new stand. Hall et al. (2008) examined dNBR values for fire disturbances in the Boreal Shield West determining that moderate and severe fires corresponded to dNBR values > 0.284.

2.3.2. Spectral forest recovery metrics

A five-year post-disturbance period was used to examine spectral forest recovery in this study with the knowledge that the initial first few years of tree species reestablishment after disturbance is critical for monitoring forest recovery (Fig. 3) (Goetz et al., 2006; Kennedy et al., 2012). Although the temporal window used to observe recovery in our research was relatively short, it allowed for partitioning of the available Landsat time series into multiple informative epochs. Kennedy et al. (2012) proposed a five-year window stating that it was critical to monitor the initiation of recovery, and this was supported by Pickell

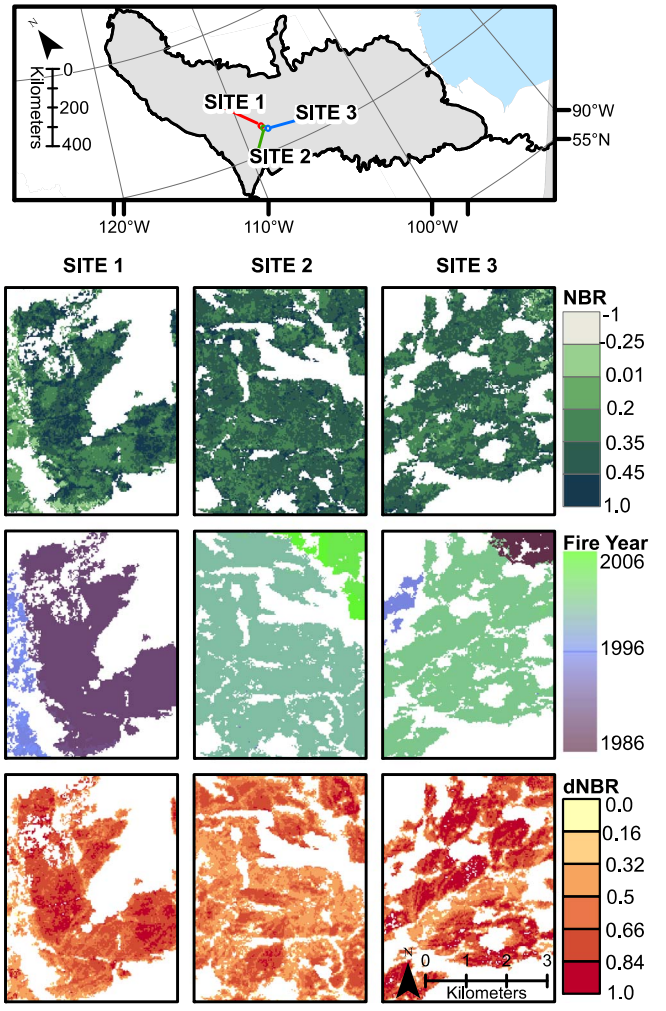

Fig. 2. Example of spectral data used for three sites in the Taiga Shield West. The first column is associated with Site 1, the second column Site 2 and the third column Site 3; this pattern is repeated in Figs. 3 & 7, and each site represents an area affected by a fire that occurred in the early, middle or later periods of the time series respectively. The top row shows the pre-disturbance NBR values, while second row shows which year fire occurred. The bottom row shows the dNBR values for each fire year.

et al. (2016) who showed spectral signals tend to saturate and match that of pre-disturbance values rapidly following disturbance. Likewise Schroeder et al. (2011) found post-disturbance recovery of NDVI & TCA returning back to an undisturbed range around 5 years and NBR within 7 years after fire. Lastly, the work of Gauthier et al. (2015) provides supporting insights, as they state that observing the initial period of forest recovery (while not noting how long or exactly when) is informative upon the ultimate return of forests.

The first metric calculated was the Relative Recovery Indicator (RRI) which is a modified version of the Recovery Indicator (RI) that was used by Kennedy et al. (2012) to compare the spectral disturbance magnitude to the recovery magnitude five years post disturbance. We modified it to work with our unfitted spectral trajectory data (Fig. 4) and is calculated as:

$$RRI = \frac{ARI}{\Delta NBR_{disturbance}}$$

where $\Delta NBR_{disturbance}$ is the change in NBR due to disturbance. We modified the RI to utilize the maximum NBR value from year four or five, calculated as:

$$\text{Absolute Recovery Indicator (ARI)} = \text{Max}\,(NBR_{Y+5}, NBR_{Y+4}) - NBR_{Y0}$$

where $\text{Max}(NBR_{y+5}, NBR_{y+4})$ is the maximum of either NBR value

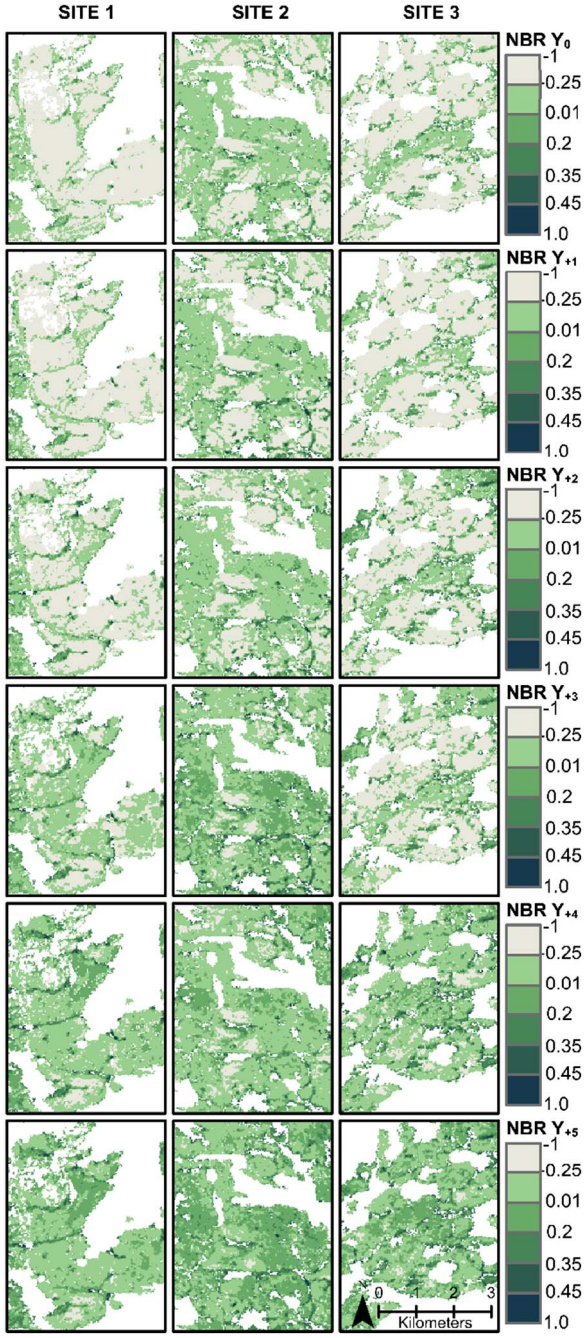

Fig. 3. For the same three sites shown in Fig. 2 (Site 1, Site 2, and Site 3), NBR time series from the year of disturbance to five years after are shown, with time since disturbance increasing from the top row to the bottom of the rows. Generally, NBR increases with time since disturbance.

four or five years after disturbance, and NBR_{y0} is the NBR value the year disturbance occurred. The maximum value from four or five years after disturbance was used in order to better accommodate our unfitted post disturbance spectral data.

The RI was originally defined using the results of the temporal segmentation, which are most often named fitted values. To capture typical pre-disturbance conditions in our unfitted spectral data, we modified $\Delta NBR_{disturbance}$ to use the average of NBR values from two years before disturbance and is calculated as:

$$\Delta NBR_{disturbance} = NBR_{pre} - NBR_{Y0}$$

where NBR_{pre} is the average NBR value from two year pre-disturbance

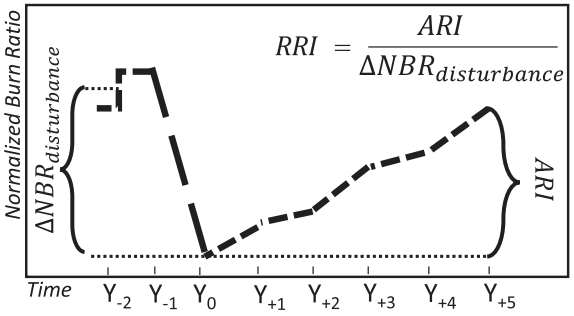

Fig. 4. The Relative Recovery Indicator (RRI), adapted from the Recovery Indicator (RI) (Kennedy et al., 2012), utilized the average of two years pre-disturbance NBR values to determine a pre-disturbance condition. The predisturbance condition is reduced by the NBR value of the year of disturbance to create a magnitude of change as shown by the term $\Delta NBR_{disturbance}$. The Absolute Recovery Indicator (ARI) is calculated as the maximum NBR value from four or five years post-disturbance reduced by NBR value from the year of disturbance.

and is calculated as:

$$NBR_{pre} = \frac{(NBR_{Y-2} + NBR_{Y-1})}{2}$$

where NBR_{y-2} and NBR_{y-1} are the NBR values from two years each before disturbance. Unique to the RI and our RRI metric is the scaling that occurs as spectral recovery is based on the amount (magnitude) of disturbance, which can be related to fire severity (Hall et al., 2008) The resultant scaling effect can be helpful in areas like the boreal that have diverse and heterogeneous signals before and after disturbance. For instance, the RI metric has been used to detect differences in spectral forest recovery across forest ownership, climate, and substrates (Kennedy et al., 2012). A value of zero indicates that no spectral forest recovery has taken place, while one indicates that an equal amount of spectral forest recovery and disturbance has occurred. Values greater than one indicate that more spectral forest recovery has occurred than spectral forest disturbance, and RI and RRI values practically range between zero and two.

Ratio of Eighty Percent (R80P), adapted from Pickell et al. (2016) was the second metric calculated, and represented the number of years required for a disturbed pixel to return to 80% of the pre-disturbance NBR value (Fig. 5). For this study, the metric was modified to be a ratio of the spectral value five years post-disturbance compared to 80% of the pre-disturbance average of the NBR values from the two preceding years, and represents the amount of spectral recovery relative to the pre-disturbance condition and is calculated as:

$$R80P = \frac{Max\,(NBR_{Y+5}, NBR_{Y+4})}{NBR_{pre}{}^{*}.\,8}$$

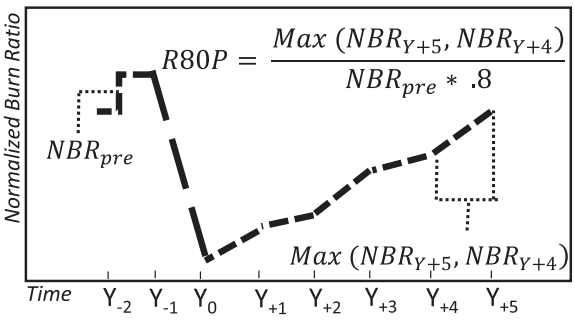

Fig. 5. The Ratio 80% of Pre-disturbance (R80P) values were adapted from Pickell et al. (2016). Additionally, the NBR_{pre} term in the denominator was calculated as the NBR average of two years prior to disturbance; that term is then multiplied by 0.8. The numerator (Max ($NBR_{(Y+5)}$, $NBR_{(Y+4)}$) is determined by obtaining the maximum NBR value from four or five years after disturbance.

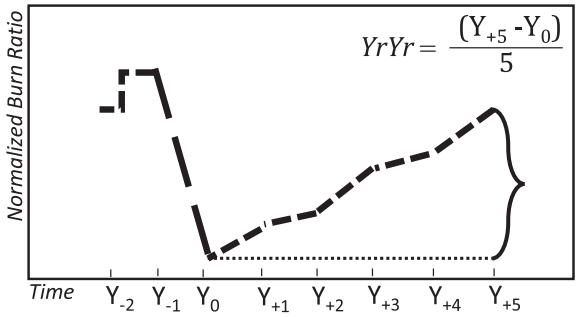

Fig. 6. The Year on Year Average (YrYr) created for this study, and is the average annual post-disturbance change in a spectral index for after five years. The terms Y_{+5} and Y_0 are the NBR from the five years after and the year of disturbance.

where the maximum NBR value from four or five year post-disturbance is used. This recovery rate metric is different from the RRI in that it gauges the amount of spectral recovery by the spectral signal that existed before disturbance. This scaling can contextualize the spectral recovery by relating the post-disturbance conditions to pre-disturbance conditions. The R80P metric as used by Pickell et al. (2016) was able to distinguish spectral recovery differences between biogeoclimatic zones, suggesting either differing pre-disturbance conditions or forest recovery processes occurring during their time series. Interpretation of R80*P* values is similar to the RRI, with a value of zero indicating that spectral forest recovery did not occur, while a value of one indicates that NBR values have recovered to be equivalent to 80% of the pre-disturbance values. Values greater than one indicate that spectral forest recovery has exceeded that of the 80% of pre-disturbance threshold.

The final metric was Year on Year Average (YrYr) which is an average rate of spectral change from the year of disturbance to the fifth post-disturbances years (Fig. 6) and is calculated as

$$YrYr = \frac{NBR_{Y+5} - NBR_{Y0}}{5}$$

where NBR_{y0}, and NBR_{y+5} are NBR values from the year disturbance occurred and five years post-disturbance as denoted by their subscript. This metric is important because it only considers spectral recovery and is neither referenced to the disturbance magnitude, nor the pre-disturbance values unlike the RRI and R80P metrics. Critical to this metric, greater NBR values are generally related to increasing forest structure and canopy cover (Wulder et al., 2009). This metric provides an insight on the average annual change after disturbance and can help capture annual post-disturbance growth. A YrYr value of zero indicates that for the five year average, zero spectral forest recovery had occurred, while positive values indicate the average gain in NBR in five years that occurred.

Three spectral forest recovery rate metrics were calculated on a yearly basis (per-pixel) using a five year recovery window. The three metrics used in this research were selected due to their ability to gauge different aspects of spectral recovery as to provide different possible methods to spectrally measure forest recovery. For instance, the RRI compares the spectral recovery magnitude to the spectral disturbance magnitude, e.g. the metric is anchored by disturbance amounts, with the disturbance magnitude quantified in terms of dNBR, which can be related to fire severity (Hall et al., 2008). Likewise, recovery magnitude has been shown to be related to forest structure throughout the recovery period (Pflugmacher et al., 2012). In contrast to the RRI, recovery using the R80P metric is related to pre-disturbance values. Because NBR values have been used to predict canopy cover (Kennedy et al., 2012) and forest structure (Frazier et al., 2014), those pre-disturbance NBR values are then a critical measure of spectral forest recovery. As opposed to evaluating recovery based on pre-disturbance conditions, the YrYr metric is calculated as the average year-to-year NBR change for five years after disturbance. These three metrics

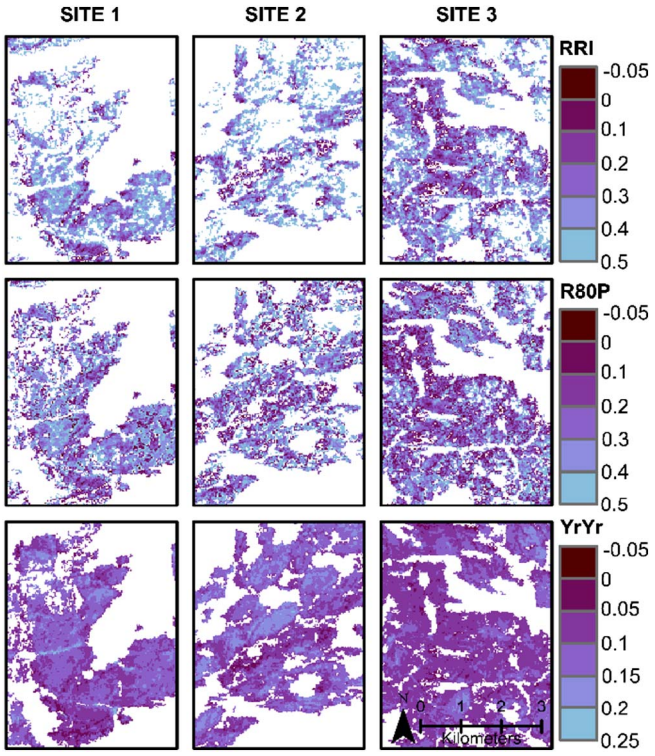

Fig. 7. Sample of spectral forest recovery metrics calculated for the same areas (Site 1, Site 2, Site 3) shown in Figs. 2 and 3, arranged in columns. Note that the YrYr values are lower than the other metrics, and class divisions are adjusted accordingly.

contextualize the measured spectral forest recovery differently, possibly providing separate insights into post-disturbance boreal forest recovery.

Areas that experienced a disturbance before 1986 or after 2006 were removed; either an insufficient amount of spectral data existed before disturbance to establish a spectral trend or not enough spectral data existed after disturbance to assess spectral recovery in our five year window (Fig. 7). The annual pre-disturbance values, dNBR values, and the spectral forest recovery rates were then averaged to create a time series for each metric for each ecozone analysis unit as well as each 100 km cell, which were then each subjected to statistical testing for trend detection.

2.3.3. Trend detection

A Theil-Sen slope estimator was used to determine the average yearly change of the pre-disturbance values, dNBR fire severity, and spectral forest recovery rates over time. A Mann-Kendall test was then used to determine whether a time series exhibited a significant monotonic increasing or decreasing trend ($p < 0.05$). Non-significant trends were considered unimportant and discarded from further analysis, although their Theil-Sen slopes are still displayed in the results for completeness. Only Mann-Kendall significant Theil-Sen slope results are reported on in the results section. Additionally, 100 km cell and ecozone analysis unit time series with five or less fire disturbances were determined to have an insufficient quantity of data to test for recovery rate trends.

Non-significant results for any of the spectral forest recovery metric time series only indicate that the rate at which forests are spectrally recovering in that cell have not changed consistently over time. Static spectral forest recovery rates or a failure of a post disturbance forest to recover cannot be indicated by a non-significant result. However, a non-significant result does indicate that either the rates of spectral forest recovery do not change greatly over time or that those rates have changed erratically and do not show a consistent trend.

Time series of annual average pre-disturbance NBR and dNBR were tested to determine if spectral recovery rates might be increasing as a result of a general NBR gain over time or increased disturbance magnitudes, which could affect the spectral recovery rates. Spectral forest recovery rate metric time series were then tested for significant trends. A significant trend in spectral forest recovery rates indicates that the rate at which vegetation is recovering within the cell is consistently changing over time, with direct impacts for productivity and sustained health. Results from both statistical tests were first assessed at the 100 km grid scale and then by each ecozone analysis unit.

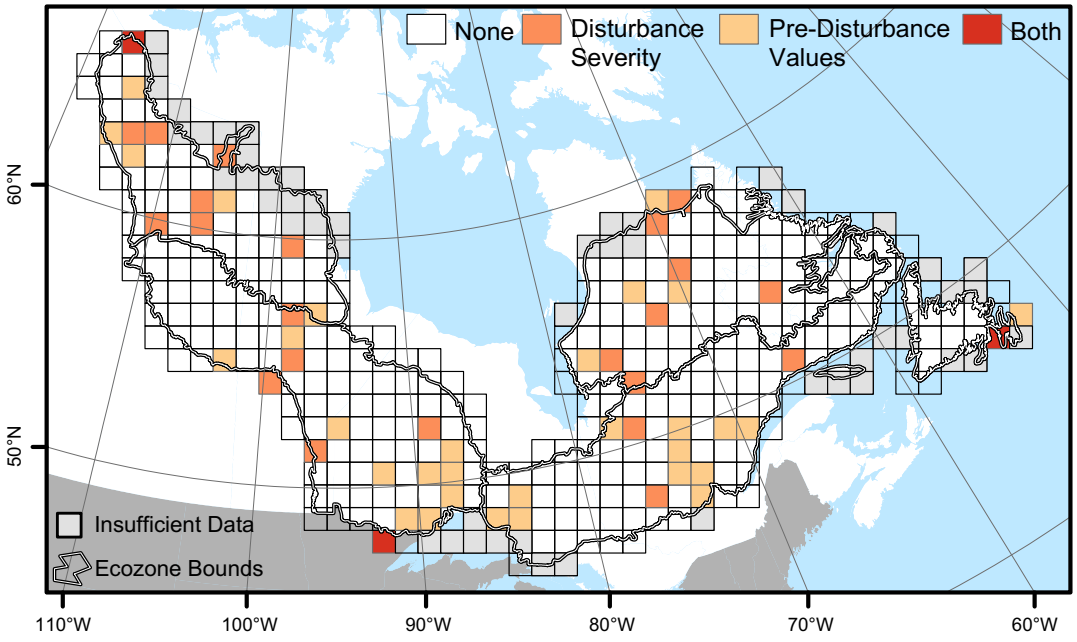

Fig. 8. Presence of significant trends over time in either pre-disturbance values or disturbance severity in the 100 km grid cells. A trend in pre-disturbance values indicates that NBR values before disturbance either increase or decrease consistently, while a trend in disturbance severity indicates that dNBR values have either increased or decreased over time.

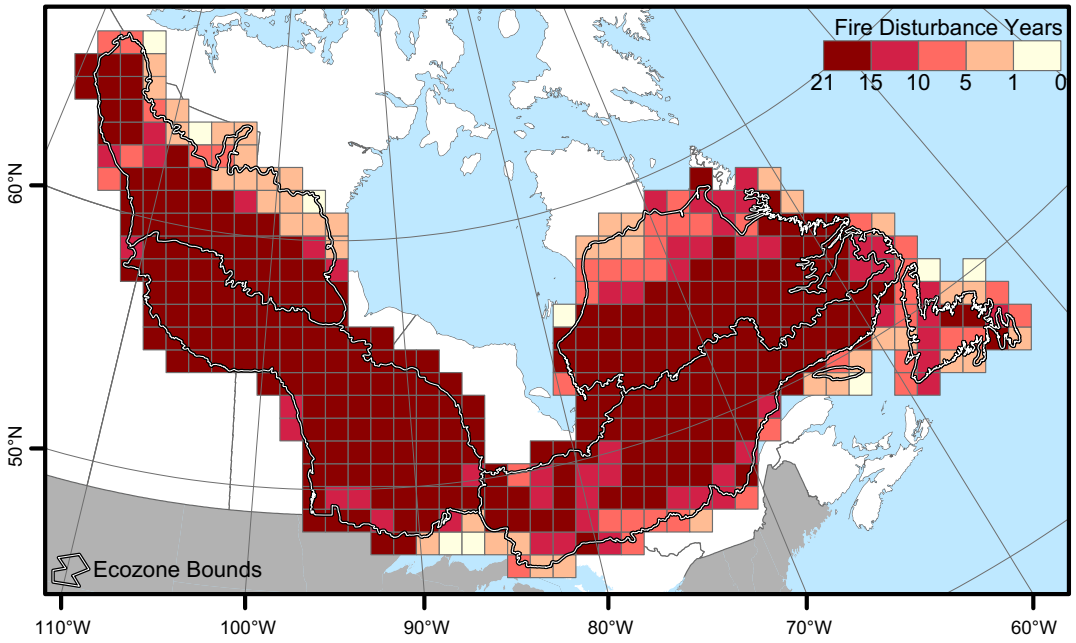

Fig. 9. The total number of years that a cell experienced a moderate or high severity fire disturbance within the time series.

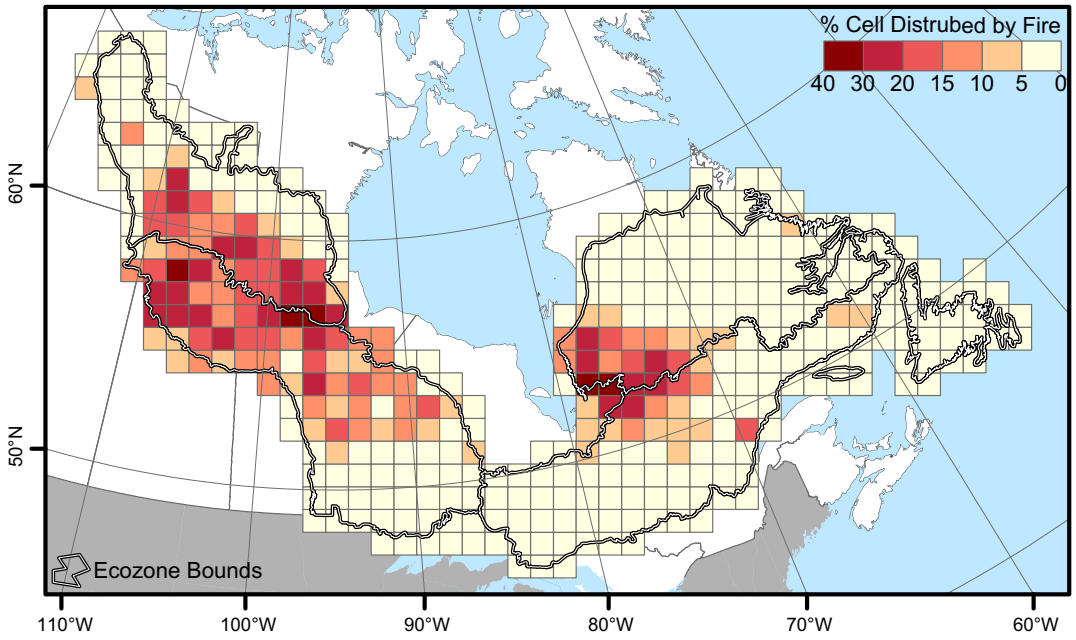

Fig. 10. The area of each grid cell that was affected by a moderate or high severity fire within the time series, shown as a percent of total area.

3. Results

3.1. Non-recovery trends, fire frequency and extent

Average pre-disturbance NBR values and NBR disturbance severity time series trend detection results are shown in Fig. 8. Approximately 85% of cells had no significant trend in NBR pre-disturbance values and no significant trend in disturbance severity over time. The remaining cells either exhibited a trend in pre-disturbance values (8.1%) or a trend in disturbance severity (5.7%) or very rarely both (0.1%). Interestingly, the cells that reported a disturbance severity trend average a very small Theil-Sen slope of − 0.000399 per year, indicating that NBR assessed severity has slightly declined over time, but not to a large degree. Conversely, the cells that produced a trend in pre-disturbance average values contain a very small positive Theil-Sen slope of 0.000191, suggesting that a very small increase in NBR values over time has occurred in those cells. These results should not alter the recovery rate metrics time series as they both represent a very small change over time. When compared to the possible range of NBR, the dNBR fire severity and pre-disturbance value, the estimated Theil-Sen slopes represent 0.05% and < 0.01% average yearly change, respectively.

The number of fire-affected years and percent area disturbed by fire throughout the time series for each 100 km grid cell is presented in Figs. 9 and 10. As expected there are more moderate and severe fires and more area burnt in western than eastern ecozone analysis units. Eighty percent of grid cells exhibited 10 or more years of fire, and overall 35% of all cells experienced between 10 and 15 years of fire in their time series. Although 97% of all grid cells experienced fire, 78% of the grid cells had < 10% of their area burnt, and only 1% of all cells recorded > 30% burnt area.

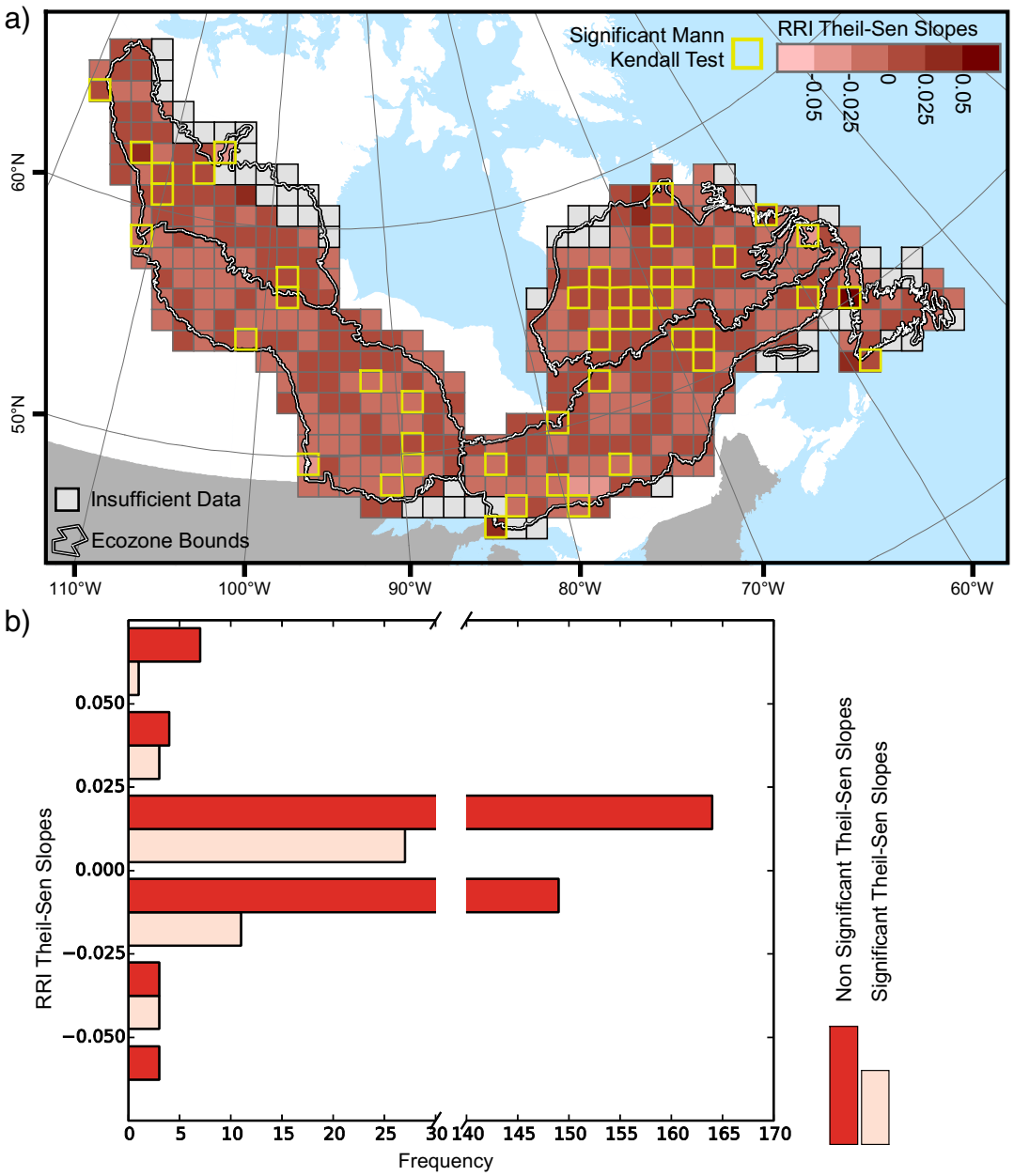

Fig. 11. Significant trending grid cells and Theil-Sen Slopes for the Relative Recovery Indicator (RRI) metric time series. a) Cells with significant Mann-Kendall results are outlined in thick gold borders, indicating a trend over time is present for that metric. Grey areas indicate that an insufficient amount of data was available to calculate a trend. b) A histogram of significant and non-significant slopes is also displayed. (For interpretation of the references to colour in this figure legend, the reader is referred to the web version of this article.)

3.2. 100 km grid spectral forest recovery rate trend

The cell-based Theil-Sen regression slopes and significant Mann-Kendall test results for the RRI metric time series are shown in Fig. 11. Overall 13% of cells with sufficient data (more than five years of fire disturbances occurring between 1986 and 2006) report a significant trend, and 69% of all significant cells contain a positive Theil-Sen slope. The largest proportion of significant trending cells (60%) contain a slope between 0.0 and 0.025 (RRI/Yr), with an average slope among them of 0.0178. This indicates that RRI values, which measure the rate of spectral recovery, were larger at the end of the time series then the beginning. Since RRI can only practically range between 0 and 2, the average RRI rate is increasing by 0.89% yearly for those positive and significant trending cells. Interestingly, 20% of all the cells in the Taiga Shield East are significant and positively trending, which is the highest proportion of any ecozone. Significant negative trends also exist, although the majority of those RRI based Theil-Sen slopes are between 0 and − 0.025.

For the R80P time series (Fig. 12), only 9% of cells with sufficient data reported a significant recovery rate trend and 70% of those significant cells contain positive Theil-Sen slopes. The majority (55%) of significant slopes range between 0.0 and 0.025, with an average yearly increase of 0.01565. This shows that R80P values among those cells increase by 0.01565 NBR units annually throughout the time series, indicating that the rate of spectral forest recovery is increasing with time for those positive and significant cells. Similar to the spatial pattern shown for the RRI results, the Taiga Shield East contains the highest proportion of significant trending cells.

YrYr grid cell time series results show significant trends (Fig. 13) in 13% of all cells, with 64% of significant grid cells having a positive slope. All positive significant slopes average 0.0021 NBR units annually, indicating the difference between NBR recovery rates are on

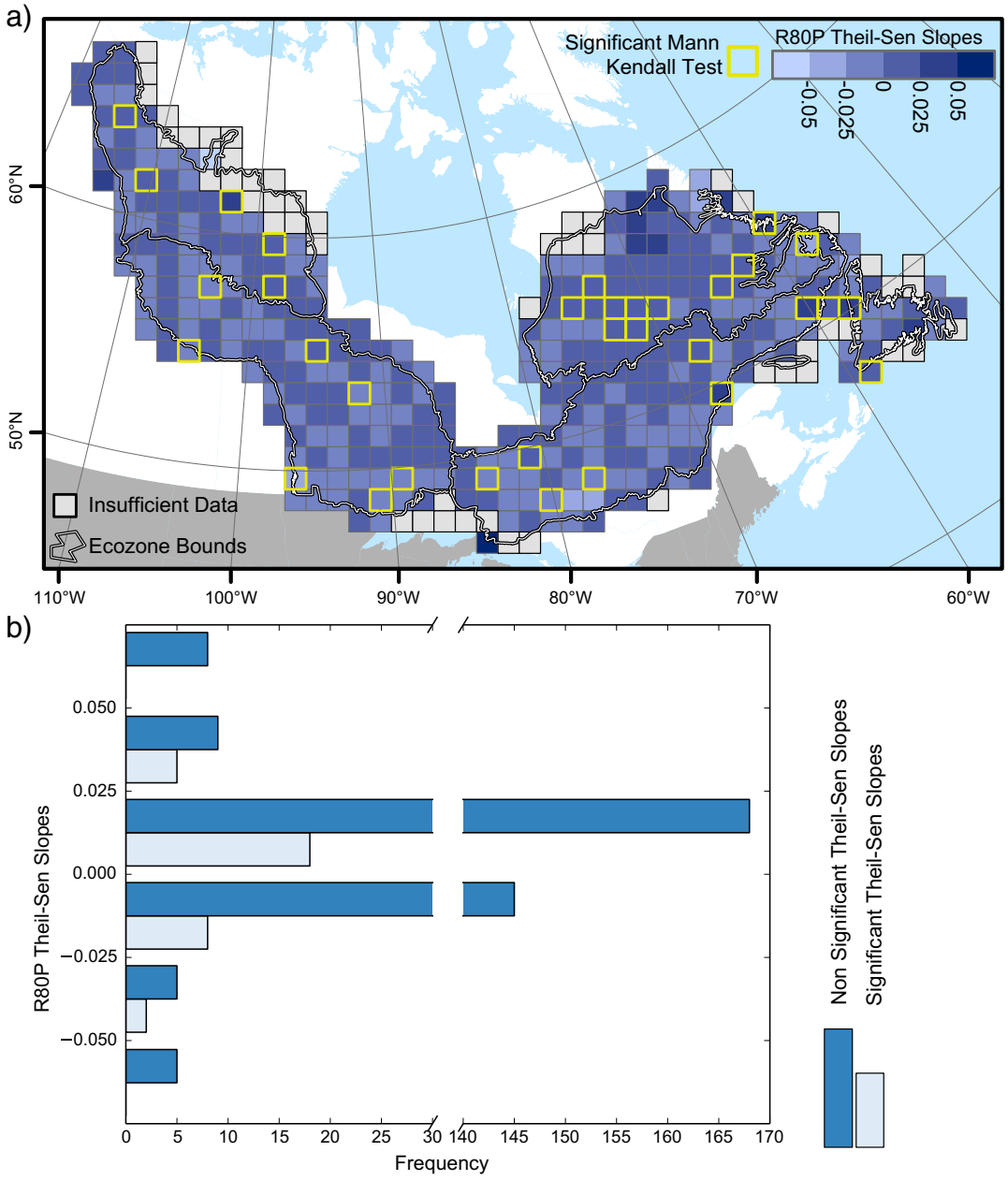

Fig. 12. Significant trending grid cells and Theil-Sen Slopes for the Ratio 80% (R80P) of Pre-disturbance grid cell time series Theil-Sen slopes are displayed. a) Cells with significant Mann-Kendall results are outlined in thick gold border, indicating a trend over time is present for that metric. Grey areas indicate that an insufficient amount of data was available to calculate a trend. b) A histogram of significant and non-significant slopes is also displayed. (For interpretation of the references to colour in this figure legend, the reader is referred to the web version of this article.)

average 0.0021 higher from year to year for those cells. Again, a contiguous pattern of significant grid cells is located in the Taiga Shield East, with that ecozone containing the majority (32%) significant cells, and significant cells occupying 21% of all cells in the ecozone.

The combination of all significant trend results across the three metrics shows two general areas where significant increasing trends tend to spatially cluster (Fig. 14). First, as previously shown in Figs. 11, 12 and 13, a contiguous block of significant cells is located in the Taiga Shield East near 70°W and 55°N. Grid cells reporting at least one significant trend occupy 26% of all cells in that ecozone. Interestingly, 25% of grid cells in the Taiga Shield West ecozone report at least one significant trend; however, no cells report significant trends for all three time series of spectral forest recovery rates. Moran's I spatial autocorrelation results show that the significant metrics are clustered over the study area (Table 1). Both Eastern ecozone analysis units had a significant clustered pattern, but the Western ecozones had non-significant and random patterns of significant recovery rate trends.

3.3. Ecozone-level analysis

The annual NBR pre-disturbance average and disturbance magnitude time series for each the ecozone analysis units showed no significant trend over time, except for the Boreal Shield West. The Boreal Shield West pre-disturbance value time series had a significant trend with a very small negative Theil-Sen slope (−0.00063 NBR units). That small negative slope value is 0.03% of the whole range of NBR and could affect R80P or RRI time series, but not the YrYr recovery metric time series.

Neither the Boreal Shield East nor West ecozone analysis units had a significant trend for any of the three spectral recovery rate metrics

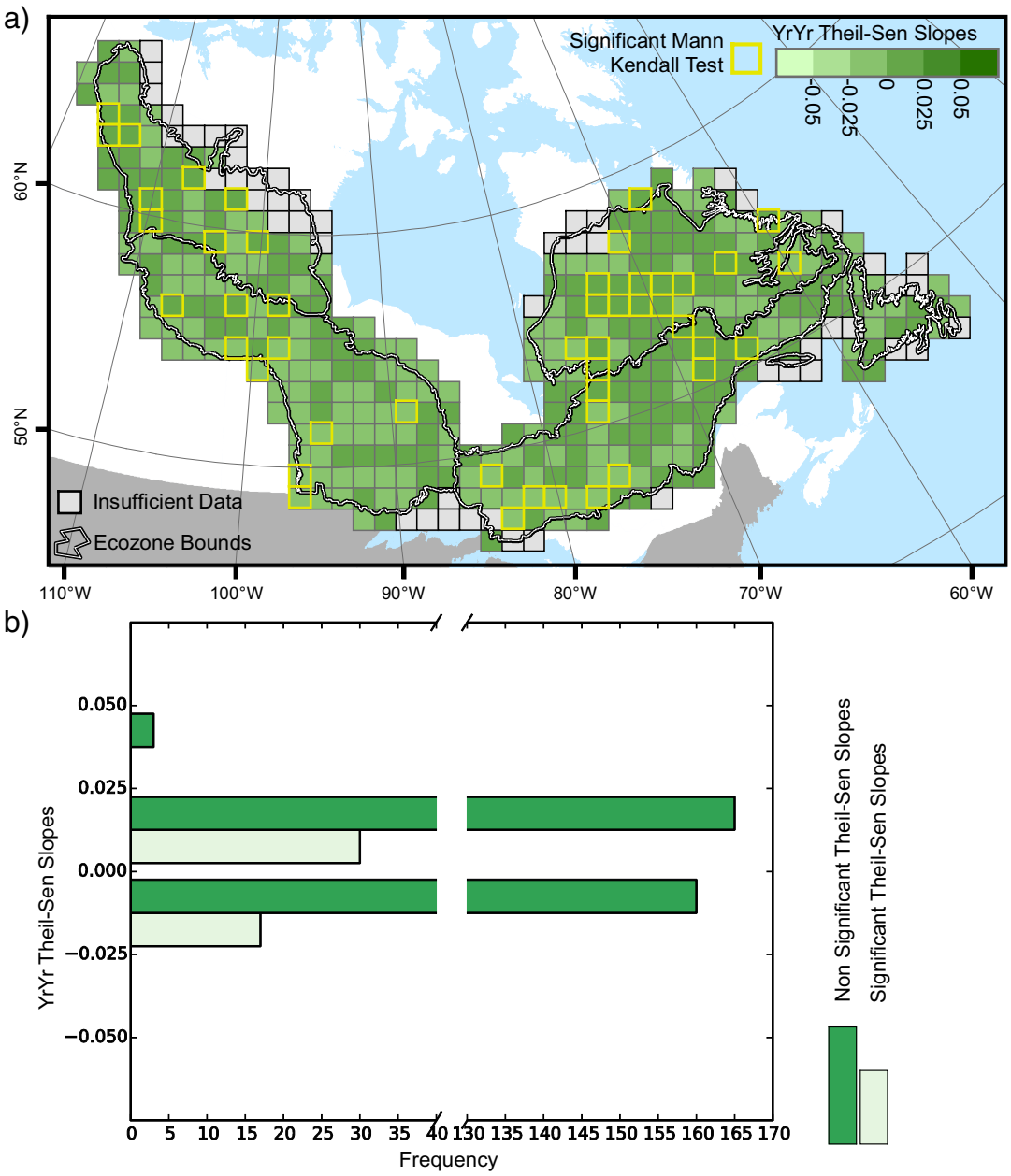

Fig. 13. Theil-Sen slopes for the Year on Year Average (YrYr) time series are displayed. a) Mann-Kendall significant trending grid cells are outlined in thick gold borders, indicating a trend over time is present for that metric. Grey areas indicate that an insufficient amount of data was available to calculate a trend. b) A histogram of significant and non-significant slopes is also displayed. (For interpretation of the references to colour in this figure legend, the reader is referred to the web version of this article.)

(Fig. 15). In contrast, the Taiga Shield East had a significant and positive trend for the R80P rates time series (Fig. 15). Theil-Sen analysis confirmed that the R80P recovery rate values increased by a total of 18% over the 26 year period. Likewise, the Taiga Shield West ecozone showed significant positive trends for the RRI and YrYr recovery rate time series. Theil-Sen analysis of the RRI time series showed a 9% increase in spectral forest recovery rates when start and end values were compared. The YrYr Theil-Sen slope value indicated that the spectral recovery rate was 12% greater at the end of the time series than the beginning. Most importantly, these significant results for the Taiga Shield West and East indicated that the rate of spectral forest recovery consistently increased over time for the ecozone.

4. Discussion

4.1. Spectral Forest recovery rate trends

We examined three different metrics of post-fire spectral forest recovery rates to determine the existence of short-term trends. Our objective was to determine if spectral recovery rates showed a consistent year to year increase or decrease. Our results showed that annual spectral forest recovery rates consistently increased over time for a portion of the 100 km cells and also for two (Taiga Shield East and West) of four ecozone analysis units. A change in spectral forest recovery rate can be crucial to future sustained boreal forest health, because any change in forest recovery rates could indicate important changes to annual growth, productivity, and essential ecosystem services provided by Canadian boreal forests (Gauthier et al., 2015).

The 100 km grid cell results display an array of significant and non-

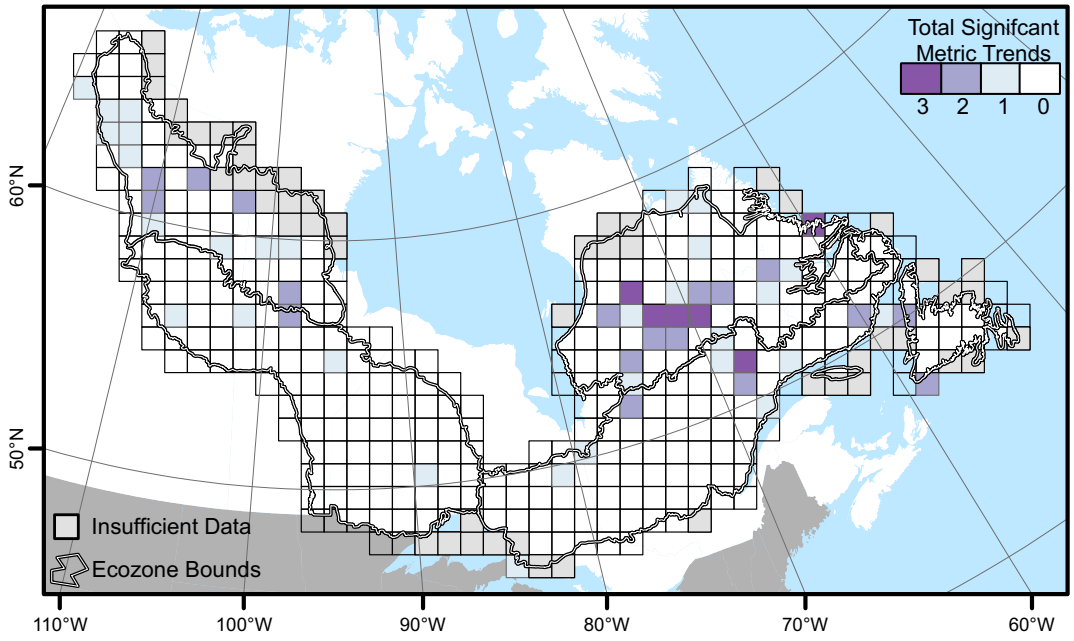

Fig. 14. Number of significant trends in a grid cell, across all spectral forest recovery time series Mann-Kendall results.

Table 1
Global Moran's I spatial autocorrelation results indicating that dispersed, random, or clustered pattern exists in the total number of significantly trending metrics.

	Global Moran's I	Z score	P value	Result
Boreal Shield East	0.16	2.85	0.00	Clustered
Boreal Shield West	− 0.05	− 0.64	0.52	Random
Taiga Shield East	0.29	4.00	0.00	Clustered
Taiga Shield West	0.09	1.23	0.22	Random
All cells	0.24	6.74	0.00	Clustered

significant spectral forest recovery rate trends that confirm spectral forest recovery rates are not fixed over time or across space. Those significant trends suggest an acceleration of spectral recovery over time for some areas of the boreal forest. In contrast to 100 km cell results, the Boreal Shield ecozone analysis units did not report any trend in spectral forest recovery rates. However, the Taiga Shield ecozone analysis units collectively had significant and positive trends for all three spectral forest recovery rate time series. The positive trend detected in the Taiga Shield East R80P time series and the positive trends detected in the RRI and YrYr Taiga Shield West time series indicate that spectral forest recovery rates have increased over time. Interestingly, the 100 km grid cell results showed a high number of significant metric trends detected in the Taiga Shield East, though when the entire Taiga Shield East ecozone analysis unit was tested only one metric showed a significant trend over time. This can indicate that when 100 km areas of significant and non-significant trends were combined across the entire Taiga Shield East significant trends in spectral recovery rates can be obscured. Thus, the 100 km grid cells were able to show spectral recovery rate trends on more of a local level than that ecozones scale.

The distribution of significantly trending spectral forest recovery rates across the 100 km grid cells with each ecozone unit showed a clustered pattern within the Taiga Shield East and Boreal Shield East, but not in the Boreal and Taiga Shield West. This suggests that the drivers of vegetation recovery, and in turn spectral recovery, were spatially concentrated, e.g. the Taiga and Boreal Shield East. When all the grid cells were subject to a Moran's I test together, the results showed that there was a clustered pattern of significantly trending spectral forest recovery rate metrics. This is suggestive of an uneven change in the drivers of vegetation recovery, as detected throughout our time series.

4.2. NBR & spectral forest recovery rate metrics

This study focused on the initial forest reestablishment and regrowth period that has been identified as a critical phase for assessing the continued health of the boreal forest, allowing for inference related to the altered growth conditions that are expected as a function of a changing climate (Gauthier et al., 2015). We examined an initial post-disturbance five-year recovery period over a 26-year time series using spectral recovery metrics based on NBR. Broadly, spectral forest recovery metrics aim to quantify the spectral change after disturbance by using a spectral vegetation index that indirectly assesses the quality and quantity of vegetation (Chu and Guo, 2013).

This study used the NBR spectral index which primarily responds to chlorophyll content and moisture in leaves (Key, 2006) with higher NBR values indicating greater quantities of vegetation in boreal forests (Wulder et al., 2009; Schroeder et al., 2011). Previously, NBR has been successfully used to detect and classify disturbances (Hermosilla et al., 2016; Hermosilla et al., 2015b; Schroeder et al., 2011), as well as inform on the age and structure of recovering forests (Pflugmacher et al., 2012). Moreover, McCarley et al. (2017), found that dNBR, "accurately detected change in canopy cover" when compared to multi-temporal LIDAR estimates of canopy cover change. Earlier work using pre- and post-fire LIDAR to characterize changes in forest structure completed by Wulder et al. (2009) further reinforces the relationship of NBR and dNBR and change in boreal forests. In that study, post-fire changes in vegetation fill, absolute change in crown closure, and relative change in mean canopy height derived from LIDAR were found to be significantly correlated with post-fire NBR, and dNBR. Furthermore, NBR has most recently been used to quantify nationwide forest disturbance and recovery on an annual basis throughout boreal Canada (White et al., 2017). However, caution is still urged when interpreting spectral forest recovery metrics, as they may not be directly related to some physical forest recovery indicators (Kennedy et al., 2012; Frolking et al., 2009).

The many increasing and decreasing NBR-based recovery rates found in this study could be a result of a number of factors currently affecting the Canadian boreal. Warmer temperatures are reported to provide more favorable conditions in some areas for black spruce dominated boreal forests, while at the same time hindering or

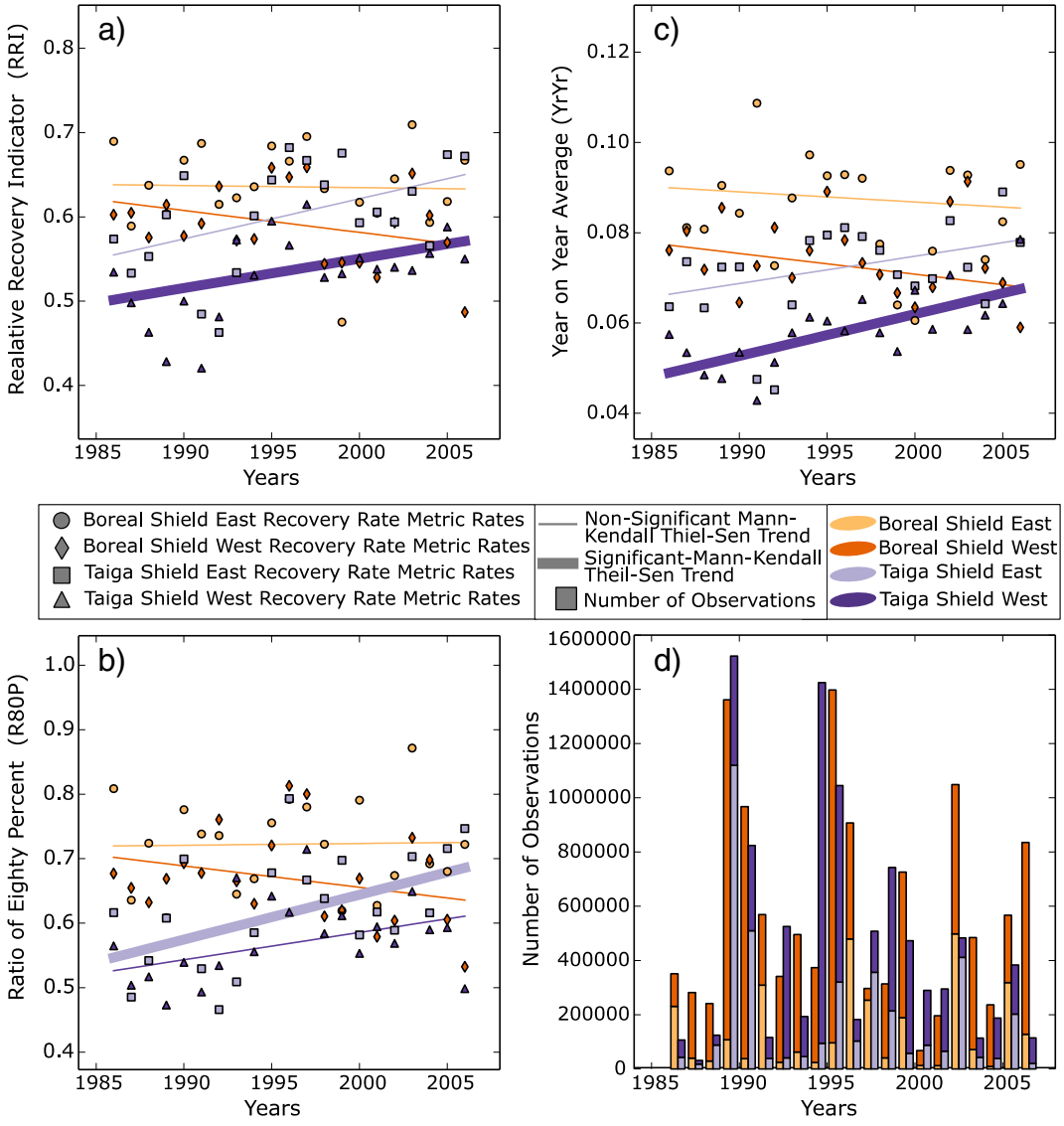

Fig. 15. Relative Recovery Indicator (Panel A), Ratio 80 Percent (Panel B), and Year on Year Average (Panel C) is displayed by ecozone, as well the Theil-Sen regression displaying a significant Mann-Kendall trend denoted by a thicker line. Non-Significant Mann Kendall -Theil-Sen Trends are shown with a thin line in the preceding panels. Panel D shows the number of pixels per year for each ecozone that were used in the subsequent five spectral recovery period.

preventing growth in other areas (D'Orangeville et al., 2016). Another factor affecting the NBR based recovery rates is the already noted productivity changes occurring throughout the boreal that correspond to increased amounts of photosynthetic vegetation (Nemani et al., 2003; Jarvis and Linder, 2000). In addition, a lengthening growing season can and will directly affect seedling reestablishment and annual growth (Lemprière et al., 2008; Colombo, 1998). Furthermore, any change in disturbance characteristics directly impacts the capability of boreal tree species to re-establish in a disturbed area (Stocks et al., 1998; Flannigan et al., 2000; Flannigan et al., 2005; Johnstone et al., 2010). Lastly, biotic factors, like that of large herbivore herding patterns, can affect seasonal growth over large areas causing heterogeneous effects on recovering vegetation (Chubbs et al., 1993, Bechtel et al., 2004, Johnson et al., 2003, Courtois et al., 2007, Rickbeil et al., 2017).

Our spectral recovery results build upon previous research efforts that have aimed to assess the recovery of boreal forests using Landsat time series. Fraser et al. (2014a, 2014b) examined recovery resulting from fire disturbances in Canadian boreal forests and found that multiple spectral vegetation indices increase with time since disturbance. Similarly, Ju and Masek (2016) observed areas recovering from fires primarily showed an increase in NDVI related to accumulating recovering vegetation which they noted in their North American study of Landsat-based time series study. Further, Pouliot et al. (2009) found that spectral recovery rates varied over time in Canadian boreal forests, although their study only applied to a limited area. These results compare favorably to our results that indicated spectral forest recovery rates are not fixed over time or across space in the Boreal and Taiga Shield East and West ecozones.

4.3. Changing conditions warrant continued boreal monitoring

The current black and white spruce forests of the Taiga Shield and Boreal Shield ecozones are a patchwork mosaic of ages, compositions, structures, biodiversity, and productivity (Brandt, 2009; Ecological Stratification Working Group, 1996). Fire is an integral part of these forests, and often severe enough to remove a stand and initiate regeneration (Weber and Flannigan, 1997; Pickell et al., 2016). Adding to this complexity is that post-disturbance recovery can follow multiple paths affected by many localized factors, such as fire severity, pre-disturbance species composition and proximity to undisturbed patches (Chen and Popadiouk, 2002). Thus, the disturbance and recovery cycles

of the boreal forest ensure that any landscape is not static. Continued monitoring is required to enable a comprehensive understanding of ecosystem change over time.

The disturbance and recovery cycle maintaining Canadian boreal forests are affected by many agents, either working in unison and at times against each other to produce mixed and distributed effects across the landscape. The currently warming climate in the Canadian boreal (Price et al., 2013) alters numerous biotic (insects, harvest, disease) and abiotic (temperature and precipitation changes, seasonal shifts, novel disturbance characteristics) factors that can depart from long term expectations and also interact with each other. This interaction can produce a heterogeneous set of conditions where once more homogenous conditions may have previously prevailed. Most importantly, tree species capable of exploiting the new conditions can be expected to thrive, while others may decline (Gauthier et al., 2015). Remarkably, gains in annual growth due to the surmised favorable conditions (warmer temperatures) can be offset by declines caused by another factor (lack of moisture) (Brooks et al., 1998; Brandt et al., 2013; D'Orangeville et al., 2016).

5. Conclusion

In this research we used fine spatial scale Landsat time series data to examine spectral forest recovery rates over time across a large proportion (~50%) of the Canadian boreal forest as represented by the Boreal and Taiga Shield ecozones. The use of multiple metrics measuring spectral forest recovery rates allowed us to gain multiple insights into how spectral recovery can change over time. The results show the spectral forest recovery rates vary over space and time. Spectral forest recovery rate trends exist and have accelerated, indicating that the rate of post-disturbance spectral recovery has increased over time in both Taiga Shield ecozones. These results will help researchers more effectively map spectral forest recovery, recovery rates and their trends over time, while managers and decision makers should find these results useful to understand the ever changing condition of Canadian boreal forests.

Acknowledgements

We thank the USGS for open access to the Landsat imagery archive and also for making Landsat data available with a high level of preprocessing completed. This research was undertaken as part of the "National Terrestrial Ecosystem Monitoring System (NTEMS): Timely and detailed national cross-sector monitoring for Canada" project jointly funded by the Canadian Space Agency (CSA), Government Related Initiatives Program (GRIP), and the Canadian Forest Service (CFS) of Natural Resources Canada. This research was enabled in part by support provided by WestGrid (www.westgrid.ca) and Compute Canada (www.computecanada.ca). Support for this research was provided by a Natural Sciences and Engineering Research Council of Canada (NSERC) Discovery Grant RGPIN311926-13 to Coops and a University of British Columbia graduate scholarship to Frazier. Thanks are also given to multiple anonymous reviewers and editors for their constructive and insightful comments.

References

Alcaraz-Segura, D., Chuvieco, E., Epstein, H.E., Kasischke, E.S., Trishchenko, A., 2010. Debating the greening vs. browning of the North American boreal forest: differences between satellite datasets. Glob. Chang. Biol. 16 (2), 760–770.

Andrew, M.E., Wulder, M.A., Coops, N.C., 2012. Identification of de facto protected areas in boreal Canada. Biol. Conserv. 146 (1), 97–107.

Barber, V.A., Juday, G.P., Finney, B.P., 2000. Reduced growth of Alaskan white spruce in the twentieth century from temperature-induced drought stress. Nature 405 (6787), 668–673.

Bechtel, R., Sanchez-Azofeifa, A., Rivard, B., Hamilton, G., Martin, J., Dzus, E., 2004. Associations between woodland caribou telemetry data and Landsat TM spectral reflectance. Int. J. Remote Sens. 25 (21), 4813–4828.

Beck, P.S., Goetz, S.J., 2011. Satellite observations of high northern latitude vegetation productivity changes between 1982 and 2008: ecological variability and regional differences. Environ. Res. Lett. 6 (4), 045501.

Bi, J., Xu, L., Samanta, A., Zhu, Z., Myneni, R., 2013. Divergent arctic-boreal vegetation changes between North America and Eurasia over the past 30 years. Remote Sens. 5 (5), 2093–2112.

Bolton, D.K., Coops, N.C., Wulder, M.A., 2015. Characterizing residual structure and forest recovery following high-severity fire in the western boreal of Canada using Landsat time-series and airborne lidar data. Remote Sens. Environ. 163, 48–60.

Brandt, J.P., 2009. The extent of the North American boreal zone. Environ. Rev. 17 (NA), 101–161.

Brandt, J.P., Flannigan, M.D., Maynard, D.G., Thompson, I.D., Volney, W.J.A., 2013. An introduction to Canada's boreal zone: ecosystem processes, health, sustainability, and environmental issues 1. Environ. Rev. 21 (4), 207–226.

Brooks, J.R., Flanagan, L.B., Ehleringer, J.R., 1998. Responses of boreal conifers to climate fluctuations: indications from tree-ring widths and carbon isotope analyses. Can. J. For. Res. 28 (4), 524–533.

Buma, B., 2012. Evaluating the utility and seasonality of NDVI values for assessing post-disturbance recovery in a subalpine forest. Environ. Monit. Assess. 184 (6), 3849–3860.

Chen, H.Y., Popadiouk, R.V., 2002. Dynamics of North American boreal mixedwoods. Environ. Rev. 10 (3), 137–166.

Chu, T., Guo, X., 2013. Remote sensing techniques in monitoring post-fire effects and patterns of forest recovery in boreal forest regions: a review. Remote Sens. 6 (1), 470–520.

Chubbs, T.E., Keith, L.B., Mahoney, S.P., McGrath, M.J., 1993. Responses of woodland caribou (*Rangifer tarandus* caribou) to clear-cutting in east-central Newfoundland. Can. J. Zool. 71 (3), 487–493.

Colombo, S.J., 1998. Climatic warming and its effect on bud burst and risk of frost damage to white spruce in Canada. For. Chron. 74 (4), 567–577.

Courtois, R., Ouellet, J.P., Breton, L., Gingras, A., Dussault, C., 2007. Effects of forest disturbance on density, space use, and mortality of woodland caribou. Ecoscience 14 (4), 491–498.

Cuevas-González, M., Gerard, F., Balzter, H., Riano, D., 2009. Analysing forest recovery after wildfire disturbance in boreal Siberia using remotely sensed vegetation indices. Glob. Chang. Biol. 15 (3), 561–577.

D'Orangeville, L., Duchesne, L., Houle, D., Kneeshaw, D., Côté, B., Pederson, N., 2016. Northeastern North America as a potential refugium for boreal forests in a warming climate. Science 352 (6292), 1452–1455.

Ecological Stratification Working Group, 1996. A National Ecological Framework for Canada. Agriculture and Agri-Food Canada and Environment Canada, Ottawa, ON Available from. http://sis.agr.gc.ca/cansis/publications/ecostrat/cad_report.pdf [cited on Feb 2nd 2016].

Epting, J., Verbyla, D., Sorbel, B., 2005. Evaluation of remotely sensed indices for assessing burn severity in interior Alaska using Landsat TM and ETM +. Remote Sens. Environ. 96 (3), 328–339.

Flannigan, M.D., Stocks, B.J., Wotton, B.M., 2000. Climate change and forest fires. Sci. Total Environ. 262 (3), 221–229.

Flannigan, M.D., Logan, K.A., Amiro, B.D., Skinner, W.R., Stocks, B.J., 2005. Future area burned in Canada. Clim. Chang. 72 (1–2), 1–16.

Fraser, R.H., Olthof, I., Carrière, M., Deschamps, A., Pouliot, D., 2011. Detecting long-term changes to vegetation in northern Canada using the Landsat satellite image archive. Environ. Res. Lett. 6 (4), 045502.

Fraser, R.H., Olthof, I., Kokelj, S.V., Lantz, T.C., Lacelle, D., Brooker, A., ... Schwarz, S., 2014a. Detecting landscape changes in high latitude environments using Landsat trend analysis: 1. Visualization. Remote Sens. 6 (11), 11533–11557.

Fraser, R.H., Olthof, I., Kokelj, S.V., Lantz, T.C., Lacelle, D., Brooker, A., ... Schwarz, S., 2014b. Detecting landscape changes in high latitude environments using Landsat trend analysis: 1. Visualization. Remote Sens. 6 (11), 11533–11557.

Frazier, R.J., Coops, N.C., Wulder, M.A., Kennedy, R., 2014. Characterization of aboveground biomass in an unmanaged boreal forest using Landsat temporal segmentation metrics. ISPRS J. Photogramm. Remote Sens. 92, 137–146.

Frazier, R.J., Coops, N.C., Wulder, M.A., 2015. Boreal shield forest disturbance and recovery trends using Landsat time series. Remote Sens. Environ. 170, 317–327.

French, N.H., Kasischke, E.S., Hall, R.J., Murphy, K.A., Verbyla, D.L., Hoy, E.E., Allen, J.L., 2008. Using Landsat data to assess fire and burn severity in the North American boreal forest region: an overview and summary of results. Int. J. Wildland Fire 17 (4), 443–462.

Frolking, S., Palace, M.W., Clark, D.B., Chambers, J.Q., Shugart, H.H., Hurtt, G.C., 2009. Forest disturbance and recovery: a general review in the context of spaceborne remote sensing of impacts on aboveground biomass and canopy structure. J. Geophys. Res. Biogeosci. 114 (G2).

Gamache, I., Payette, S., 2004. Height growth response of tree line black spruce to recent climate warming across the forest-tundra of eastern Canada. J. Ecol. 92 (5), 835–845.

Gauthier, S., Bernier, P., Burton, P.J., Edwards, J., Isaac, K., Isabel, N., ... Nelson, E.A., 2014. Climate change vulnerability and adaptation in the managed Canadian boreal forest 1. Environ. Rev. 22 (3), 256–285.

Gauthier, S., Bernier, P., Kuuluvainen, T., Shvidenko, A.Z., Schepaschenko, D.G., 2015. Boreal forest health and global change. Science 349 (6250), 819–822.

Girardin, M.P., Hogg, E.H., Bernier, P.Y., Kurz, W.A., Guo, X.J., Cyr, G., 2016. Negative impacts of high temperatures on growth of black spruce forests intensify with the anticipated climate warming. Glob. Chang. Biol. 22 (2), 627–643.

Goetz, S.J., Bunn, A.G., Fiske, G.J., Houghton, R.A., 2005. Satellite-observed photosynthetic trends across boreal North America associated with climate and fire disturbance. Proc. Natl. Acad. Sci. U. S. A. 102 (38), 13521–13525.

Goetz, S.J., Fiske, G.J., Bunn, A.G., 2006. Using satellite time-series data sets to analyze

fire disturbance and forest recovery across Canada. Remote Sens. Environ. 101 (3), 352–365.
Hall, R.J., Freeburn, J.T., De Groot, W.J., Pritchard, J.M., Lynham, T.J., Landry, R., 2008. Remote sensing of burn severity: experience from western Canada boreal fires. Int. J. Wildland Fire 17 (4), 476–489.
Hermosilla, T., Wulder, M.A., White, J.C., Coops, N.C., Hobart, G.W., 2015a. An integrated Landsat time series protocol for change detection and generation of annual gap-free surface reflectance composites. Remote Sens. Environ. 158, 220–234.
Hermosilla, T., Wulder, M.A., White, J.C., Coops, N.C., Hobart, G.W., 2015b. Regional detection, characterization, and attribution of annual forest change from 1984 to 2012 using Landsat-derived time-series metrics. Remote Sens. Environ. 170, 121–132.
Hermosilla, T.A., Coops, N.C., Hobart, G.W., Campbell, L.B., 2016. Mass data processing of time series Landsat imagery: pixels to data products for forest monitoring. Int. J. Digital Earth 9 (11), 1035–1054.
Jarvis, P., Linder, S., 2000. Botany: constraints to growth of boreal forests. Nature 405 (6789), 904–905.
Johnson, C.J., Alexander, N.D., Wheate, R.D., Parker, K.L., 2003. Characterizing woodland caribou habitat in sub-boreal and boreal forests. For. Ecol. Manag. 180 (1), 241–248.
Johnstone, J.F., Hollingsworth, T.N., Chapin, F.S., Mack, M.C., 2010. Changes in fire regime break the legacy lock on successional trajectories in Alaskan boreal forest. Glob. Chang. Biol. 16 (4), 1281–1295.
Ju, J., Masek, J.G., 2016. The vegetation greenness trend in Canada and US Alaska from 1984–2012 Landsat data. Remote Sens. Environ. 176, 1–16.
Kennedy, R.E., Yang, Z., Cohen, W.B., Pfaff, E., Braaten, J., Nelson, P., 2012. Spatial and temporal patterns of forest disturbance and regrowth within the area of the Northwest Forest Plan. Remote Sens. Environ. 122, 117–133.
Kennedy, R.E., Andréfouët, S., Cohen, W.B., Gómez, C., Griffiths, P., Hais, M., ... Meigs, G.W., 2014. Bringing an ecological view of change to Landsat-based remote sensing. Front. Ecol. Environ. 12 (6), 339–346.
Key, C.H., 2006. Ecological and sampling constraints on defining landscape fire severity. Fire Ecol. 2 (2), 34–59.
Key, C.H., Benson, N.C., 1999. The Normalized Burn Ratio (NBR): A Landsat TM Radiometric Measure of Burn Severity. United States Geological Survey.
Kull, S.J., Kurz, W.A., Rampley, G.J., Banfield, G.E., Schivatcheva, R.K., Apps, M.J., 2006. Operational-scale Carbon Budget Model of the Canadian Forest Sector (CBM-CFS3) Version 1.0: User's Guide. 2006.
Kurz, W.A., Apps, M.J., Webb, T.M., McNamee, P.J., 1992. The Carbon Budget of the Canadian Forest Sector: Phase I. Vol. 326 Forestry Canada, Northern Forestry Centre.
Lemprière, T.C., Bernier, P.Y., Carroll, A.L., Flannigan, M.D., Gilsenan, R.P., McKenney, D.W., Hogg, E.H., ... Blain, D., 2008. The Importance of Forest Sector Adaptation to Climate Change. Vol. 416 Northern Forestry Centre.
Markham, B.L., Helder, D.L., 2012. Forty-year calibrated record of earth-reflected radiance from Landsat: a review. Remote Sens. Environ. 122, 30–40.
McCarley, T.R., Kolden, C.A., Vaillant, N.M., Hudak, A.T., Smith, A.M., Wing, B.M., ... Kreitler, J., 2017. Multi-temporal LiDAR and Landsat quantification of fire-induced changes to forest structure. Remote Sens. Environ. 191, 419–432.
McManus, K.M., Morton, D.C., Masek, J.G., Wang, D., Sexton, J.O., Nagol, J.R., Ropars, P., Boudreau, S., 2012. Satellite-based evidence for shrub and graminoid tundra expansion in northern Quebec from 1986 to 2010. Glob. Chang. Biol. 18 (7), 2313–2323.
Myneni, R.B., Keeling, C.D., Tucker, C.J., Asrar, G., Nemanill, R.R., 1997. Increased plant growth in the northern high latitudes from 1981 to 1991. Nature 386, 698–702.
Nemani, R.R., Keeling, C.D., Hashimoto, H., Jolly, W.M., Piper, S.C., Tucker, C.J., ... Running, S.W., 2003. Climate-driven increases in global terrestrial net primary production from 1982 to 1999. Science 300 (5625), 1560–1563.
Olthof, I., Latifovic, R., 2007. Short-term response of arctic vegetation NDVI to temperature anomalies. Int. J. Remote Sens. 28 (21), 4823–4840.
Olthof, I., Pouliot, D., Latifovic, R., Chen, W., 2008. Recent (1986–2006) vegetation-specific NDVI trends in northern Canada from satellite data. Arctic 61, 4381–4394.
Pflugmacher, D., Cohen, W.B., Kennedy, R.E., 2012. Using Landsat-derived disturbance history (1972–2010) to predict current forest structure. Remote Sens. Environ. 122, 146–165.
Pickell, P.D., Hermosilla, T., Frazier, R.J., Coops, N.C., Wulder, M.A., 2016. Forest recovery trends derived from Landsat time series for North American boreal forests. Int. J. Remote Sens. 37 (1), 138–149.
Pouliot, D., Latifovic, R., Olthof, I., 2009. Trends in vegetation NDVI from 1 km AVHRR data over Canada for the period 1985–2006. Int. J. Remote Sens. 30 (1), 149–168.
Price, D.T., Alfaro, R.I., Brown, K.J., Flannigan, M.D., Fleming, R.A., Hogg, E.H., ... Pedlar, J.H., 2013. Anticipating the consequences of climate change for Canada's boreal forest ecosystems 1. Environ. Rev. 21 (4), 322–365.
Rickbeil, G.J., Hermosilla, T., Coops, N.C., White, J.C., Wulder, M.A., 2017. Barren-ground caribou (Rangifer tarandus groenlandicus) behaviour after recent fire events; integrating caribou telemetry data with Landsat fire detection techniques. Glob. Chang. Biol. 23 (3), 1036–1047.
Schroeder, T.A., Cohen, W.B., Yang, Z., 2007. Patterns of forest regrowth following clearcutting in western Oregon as determined from a Landsat time-series. For. Ecol. Manag. 243 (2), 259–273.
Schroeder, T.A., Wulder, M.A., Healey, S.P., Moisen, G.G., 2011. Mapping wildfire and clearcut harvest disturbances in boreal forests with Landsat time series data. Remote Sens. Environ. 115 (6), 1421–1433.
Slayback, D.A., Pinzon, J.E., Los, S.O., Tucker, C.J., 2003. Northern hemisphere photosynthetic trends 1982–99. Glob. Chang. Biol. 9 (1), 1–15.
Stocks, B.J., Fosberg, M.A., Lynham, T.J., Mearns, L., Wotton, B.M., Yang, Q., ... McKenney, D.W., 1998. Climate change and forest fire potential in Russian and Canadian boreal forests. Clim. Chang. 38 (1), 1–13.
Stocks, B.J., Mason, J.A., Todd, J.B., Bosch, E.M., Wotton, B.M., Amiro, B.D., ... Skinner, W.R., 2002. Large forest fires in Canada, 1959–1997. J. Geophys. Res.-Atmos. 107 (D1).
Sulla-Menashe, D., Friedl, M.A., Woodcock, C.E., 2016. Sources of bias and variability in long-term Landsat time series over Canadian boreal forests. Remote Sens. Environ. 177, 206–219.
Turubanova, S., Potapov, P., Krylov, A., Tyukavina, A., McCarty, J.L., Radeloff, V.C., Hansen, M.C., 2015. Using the Landsat data archive to assess long-term regional forest dynamics assessment in Eastern Europe, 1985–2012. Int. Arch. Photogramm. Remote. Sens. Spat. Inf. Sci. 40 (7), 531.
Urquizo, N., 2000. Ecological Assessment of the Boreal Shield Ecozone. Environment Canada, Ottawa, ON.
Vogelmann, J.E., Gallant, A.L., Shi, H., Zhu, Z., 2016. Perspectives on monitoring gradual change across the continuity of Landsat sensors using time-series data. Remote Sens. Environ. 185, 258–270.
Weber, M.G., Flannigan, M.D., 1997. Canadian boreal forest ecosystem structure and function in a changing climate: impact on fire regimes. Environ. Rev. 5 (3–4), 145–166.
White, J.C., Wulder, M.A., 2014. The Landsat observation record of Canada: 1972–2012. Can. J. Remote. Sens. 39 (6), 455–467.
White, J.C., Wulder, M.A., Hobart, G.W., Luther, J.E., Hermosilla, T., Griffiths, P., ... Guindon, L., 2014. Pixel-based image compositing for large-area dense time series applications and science. Can. J. Remote. Sens. 40 (3), 192–212.
White, J.C., Wulder, M.A., Hermosilla, T., Coops, N.C., Hobart, G.W., 2017. A nationwide annual characterization of 25 years of forest disturbance and recovery for Canada using Landsat time series. Remote Sens. Environ. 194, 303–321.
Wilmking, M., Juday, G.P., Barber, V.A., Zald, H.S., 2004. Recent climate warming forces contrasting growth responses of white spruce at treeline in Alaska through temperature thresholds. Glob. Chang. Biol. 10 (10), 1724–1736.
Wulder, M., 1998. Optical remote-sensing techniques for the assessment of forest inventory and biophysical parameters. Prog. Phys. Geogr. 22 (4), 449–476.
Wulder, M.A., White, J.C., Alvarez, F., Han, T., Rogan, J., Hawkes, B., 2009. Characterizing boreal forest wildfire with multi-temporal Landsat and LIDAR data. Remote Sens. Environ. 113 (7), 1540–1555.
Wulder, M.A., White, J.C., Gillis, M.D., Walsworth, N., Hansen, M.C., Potapov, P., 2010. Multiscale satellite and spatial information and analysis framework in support of a large-area forest monitoring and inventory update. Environ. Monit. Assess. 170, 417–433.
Wulder, M.A., Masek, J.G., Cohen, W.B., Loveland, T.R., Woodcock, C.E., 2012. Opening the archive: how free data has enabled the science and monitoring promise of Landsat. Remote Sens. Environ. 122, 2–10.